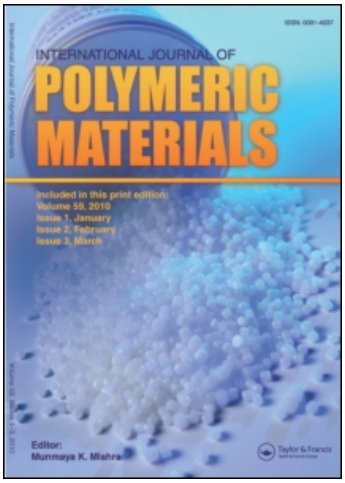

International Journal of Polymeric Materials
Publication details, including instructions for authors and subscription information:
http://www.informaworld.com/smpp/title~content=t713647664

Poly(Ethylene Terephthalate) Films with Different Content of Acid-Base Functionalities. I. Surface Modifications

Mariana Gheorghiu[a]; Mihaela Pascu[a]; G. Popa[a]; Cornelia Vasile[b]; V. Mazur[c]
[a] "Al. I. Cuza" University, Faculty of Physics, Romania [b] Macromolecular Chemistry "P. Poni" Institute, Romania [c] Metrological Center of Academy, Chisinau, Republic of Moldavia

To cite this Article Gheorghiu, Mariana , Pascu, Mihaela , Popa, G. , Vasile, Cornelia and Mazur, V.(1998) 'Poly(Ethylene Terephthalate) Films with Different Content of Acid-Base Functionalities. I. Surface Modifications', International Journal of Polymeric Materials, 40: 3, 229 — 256
To link to this Article: DOI: 10.1080/00914039808034841
URL: http://dx.doi.org/10.1080/00914039808034841

Intern. J. Polymeric Mater., 1998, Vol. 40, pp. 229–256
Reprints available directly from the publisher
Photocopying permitted by license only

Poly(Ethylene Terephthalate) Films with Different Content of Acid-Base Functionalities. I. Surface Modifications

MARIANA GHEORGHIU[a*], MIHAELA PASCU[a],
G. POPA[a], CORNELIA VASILE[b] and V. MAZUR[c]

[a]*"Al. I. Cuza" University, Faculty of Physics, RO 6600-Iasi, Romania;*
[b]*Macromolecular Chemistry "P. Poni" Institute, RO 6600-Iasi, Romania;*
[c]*Metrological Center of Academy, Chisinau, Republic of Moldavia*

(Received 23 July 1997)

Treatments of PET in an ion beam-low density plasma system, in oxygen, have been realised. Low energy (100–500 eV), but relatively high does ($3.0 \cdot 10^{15}$–$9.0 \cdot 10^{16}$ ions/cm^2) for ions were used. In this first part, the surface modifications of PET films (investigated by IR spectroscopy, X-ray diffraction, contact angle measurements, XPS angle resolved) are presented. Both chemical and physico-structural modifications take place simultaneous during ion beam treatments. The initial polar group content, immediately after the treatment, but more than this the physico-structural modifications like cross-linking and a restructured crystalline content determine the dynamic effects which control the ageing mechanisms.

Keywords: Ion beam; low density plasma; surface modification; cross-linking; dynamic effect; ageing mechanism

INTRODUCTION

It is well known that London-Lifshitz and Lewis acid/base interactions are among the main ones involved in interfacial forces [1]. Also, the thermodynamic work of adhesion is a measure of such interfacial forces [2], which in their turn can explain the properties of the wide variety of complex materials.

*Corresponding author.

For example, metal-polymer adhesion has been shown to be determined to a large extent by acid-base interactions, which modify interfacial bonding [3]. Although adhesion in polymer composites can arise from primary chemical bonds, from London-Lifshitz interactions across the interface or from mechanical interlocking, acid-base interactions are the most generally useful chemical forces that are available to modify interfacial bonding [4]. The selection of a biomaterial, as being biocompatible on a long-term basis, suppose besides the other criteria (damage to adjacent tissue, toxic or allergic reactions etc.), the values for its surface free energy components adsorption on biomaterials (as the earliest stage in blood coagulation) generally involves non-specific binding, depending on the local distribution of the heterogeneities on the biomaterial surface. Josefowicz and co-workers stood out that biospecific functional polymers may be obtained by random substitution of macromolecular chains with suitable chemical groups [5b].

On the other hand, the practical importance of surface modification of polymers has imposed extensive researches on the ageing of the plasma treated polymer surfaces [6–11]. Mechanisms like thermal decomposition of the modified layer, which were supposed to be responsible for the observed increase of water contact angle, were ruled out by different analysis [7]. Now it is clear that dynamic effects control the surface properties of polymers and also a possible restructuring of the mobile surface in the working environment must be taken into account [7–9].

In a previous paper it has been shown that a so called ion beam induced epitaxial crystallization (IBIEC) takes place for poly(ethylene terephthalate) films subjected to the action of oxygen ions of relative low energy (100–500 eV), but at high doses (10^{16} ion/cm^2) [12]. The mechanism is mainly controlled by the ratio between the fluence of fast atomic and molecular oxygen ions. This ratio determines the probability for the yielding of the polymer chains with critical dimensions and also the rates for the dynamic defect annealing and the defect production. The etching regimes for PET samples, as a function of ion energy and dose were also proposed.

The present paper stands out that, starting from an amphoteric poly(ethylene terephthalate) surface, basic or acidic surfaces may be created by treatments with oxygen ions of different energies and doses.

Moreover, the evolution of the surface energy components with the "ageing" time is specific for the different treated samples. This is not only due to the various types of functional groups and their content introduced immediately after treatments, but also to the distinct dynamic effects that are the results of the plysico-structural and chemical changes of the treated surfaces in the ion beam-plasma system. The first part of the paper presents data about surface modifications, while the second one will show the characteristics of the gas plasma phase together with the possible mechanisms responsible for the observed surface modifications and their change during ageing.

EXPERIMENTAL

The poly(ethylene terephthalate) (PET) film, 25 μ, Terom ® (produced in Romania) was treated in an ion beam-low density plasma system (IB-LDP), after washing in alcohol.

The experimental set up is described in detail elsewhere [5c, 12]. It consists mainly in a low density target plasma through which drifts a positive ion beam.

Typical parameters are: $9 \cdot 10^8$ cm^{-3}-density of the source plasma, 10^6 cm^{-3}-density of the target plasma, 3 eV-medium electron temperature and 0.25 eV-medium ion temperature. The average energies of the beam oxygen ions were: 100 eV, 300 eV and 500 eV. Treatments were performed at the following doses: $\delta_1 = 3.0 \cdot 10^{15}$ ions/cm^2, $\delta_2 = 1.5 \cdot 10^{16}$ ions/cm^2 and $\delta_3 = 9.0 \cdot 10^{16}$ ions/cm^2. A saturation regime for ion tracks is realised at δ_1, while for δ_2 and δ_3 a reimplantation regime is obtained [13].

For the sake of simplicity the following notation of the samples is used ε (ion energy)$-\delta$ (dose).

The polymer sample was not cooled during the treatment, that the thermal effects, due both to the ion bombardment and the radiation from the hot cathode of the target plasma, must be considered.

The following methods for surface investigation were used: free surface energy determination, IR spectroscopy, X-ray diffraction and XPS angle resolved.

The surface free energy components were determined by sessile drop technique. The reported values are the average over at least ten measurements performed on many area region of the sample surface, the typical dispersity of the values being ±2°.

Here is necessary to briefly point out some aspects concerning the notion of thermodynamic work of adhesion. In the earlier modelling of the physical interactions between molecules across the interfaces, the thermodynamic work of adhesion is given by the expression [14]:

$$W_a = \gamma_l(1 + \cos\theta) = 2[(\gamma_s^d \gamma_l^d)^{1/2} + (\gamma_s^p \gamma_l^p)^{1/2}] \quad (1)$$

where γ_s^d, γ_l^d are the dispersive component of the surface energy for solid (s) respectively liquid (l) and γ_s^p, γ_l^p are the polar ones. The second term in the right part of the equation (1) was arbitrarily assigned to "polar effect", even its magnitude seldom correlated with the dipole moments of the materials [14]. This excess contribution to the magnitude for W_a could be identified with acid-base interactions and thus [15]:

$$W_a = 2(\gamma_s^{LW} \gamma_l^{LW})^{1/2} + W_a^{ab} \quad (2)$$

where W_a^{ab} refers to the contribution of acid-base interaction.

The notions of acidity and basicity must be understood in the sense of Lewis theory (electron donor–acceptor). The formation of bonds between two molecules is made by partial or complete charge transfer. In practice, two main concepts are used to classify the acid-base strength of liquids: the Drago and Gutmann formalisms. In Drago's studies, each substance is considered exclusively acidic or basic. The possibility of an amphoteric character is therefore ignored, whereas it is taken into account in Gutman model [16].

Therefore, the acid-base contribution to the work of adhesion W_a^{ab} water-polymer, may be obtained in accord with [15]:

$$W_a^{ab} = \gamma_l(1 + \cos\theta) - 2(\gamma_s^{LW} \gamma_{probe}^{LW})^{1/2} \quad (3)$$

The surface tension of the liquid γ_l and its contact angle θ may be measured directly, while the Lifshitz-van der Waals contribution to the solid surface energy γ_s^{LW} is obtained using a non-self-associating

liquid with no acidic or basic character (i.e., a "neutral liquid") with the relation:

$$\gamma_s^{LW} = \left(\frac{\gamma_{probe}}{4}\right) \cdot (1 + \cos\theta_{probe}) \tag{4}$$

where θ_{probe} and γ_{probe} are the contact angle and surface tension respectively for neutral liquid. In terms of the LW-AB model, Young's equation can be written [17]:

$$W_a = 2[(\gamma_s^{LW}\gamma_l^{LW})^{1/2} + (\gamma_s^+\gamma_l^-)^{1/2} + (\gamma_s^-\gamma_l^+)^{1/2}] \tag{5}$$

where γ^+ and γ^- note the contribution due to the electron acceptor (Lewis acid) and donor (Lewis base) part respectively, for solid (s) or liquid (l).

Polar and dispersive component of the surface energy were determined with relation (1) and acid, base components with relation (5). The values for the surface energy components of the liquids used in this study are given in Table I.

The IR spectra were obtained on a Nicolet FTIR spectrometer (with 620 Advantage Processor).

A X-ray diffractometer HZG, operated with CoKα radiation, in standard (at high and small angles) and grazing X-ray incidence geometry, has been used. Taking into account the value for linear absorption coefficient for polymers [18], have been calculated the penetration depths of CoKα radiation as a function of the X-ray incidence angle, ω. The X-ray penetrates entire PET film sample for $\omega \geq 2°$, as can be observed from Figure 1.

The XPS spectra were obtained on a ESCALAB MkII (VG Scientific) photoelectron spectrometer, with an AlKα X-ray source, and a low energy flood gun for charge compensation. The total

TABLE I The values for the free surface energy components of the liquids used in this study [17]

	Component of the free surface energy (mN/m)			
Liquid	γ_l^{LW}	γ_l^+	γ_l^-	γ_l
water	21.7	25.5	25.5	72.8
formamide	32.0	3.0	22.4	57.4
α-bromonaphthalene	44.8	0	0	44.8

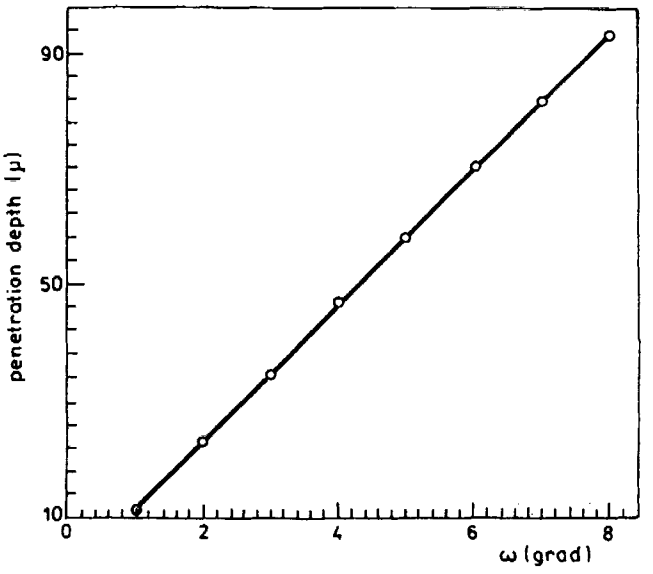

FIGURE 1 Penetration depth of CoKα in PET film sample vs. incidence angle ω.

instrumental resolution, measured as FWHM of the Ag $3d_{5/2}$ photoelectron peak, was 0.5 eV. The angle between the direction of the incident X-ray and that of observation was fixed by analyser entrance slit, 50°, while the angle between the sample surface and the direction of observation, α, was variable. Correlation between α and the sampling depth, $d = 3\lambda \sin \alpha$, is given in the Table II (λ is the inelastic mean free path for photoelectrons, which is 26 Å in polymers, at 1200 eV mean energy). It is also considered that the material is a homogeneous one.

RESULTS AND DISCUSSION

Specific Structural Features of the Untreated Polymer

The density of the film samples was 1.392 g/cm^3 and the degree of crystallinity (as determined from density data) was 65.0%.

TABLE II Correlation between α and the sampling depth d

α	22.5	37.5	52.5
d (Å)	30	47	62

The X-ray diffractogram (in Bragg-Brentano geometry) exhibits the peak due to (100) planes ($2\theta = 30°$) (Fig. 2, curve 1), for which the interplanar spacing was $d_{(100)} = 3.4478$ Å, in well agreement with literature data [18]. The enlargement of (100) peak base is due to the amorphous phase, which mainly is ascribed to the chaotically distribution of the $-CH_2-$ groups with respect to (100) benzene ring plane. The degree of crystallinity, from X-ray data, was 61.1%. The mean crystallite size perpendicular to (100) plane, was $D_{(100)} = 60$ Å.

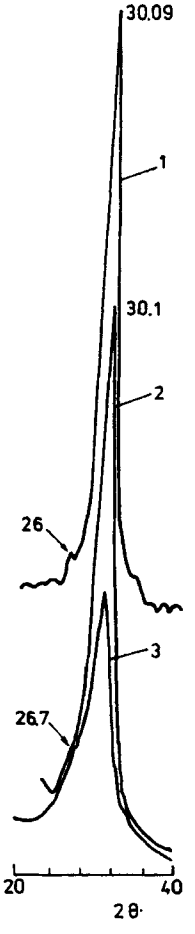

FIGURE 2 Diffractogram of the untreated PET in Bragg-Brentano geometry (curve 1) and for grazing incidence (curve 2 $\omega = 8°$, curve 3 $\omega = 4°$).

The X-ray long period, determined from small-angle scattering data, was $L = 39$ Å. As a function of ω, the (100) peak intensity is given by the number of (100) planes that have a well-defined orientation in respect with sample surface. Smaller the incidence angle ω, greater must be the angle θ for which Bragg scattering takes place. Therefore, the decrease in (100) peak intensity with the decrease of ω (Fig. 2, curves 2 and 3) shows a diminished crystallite content whose (100) planes make great angles with sample surface plane.

IR spectra for untreated PET film is similar to that for PET with high crystalline content, but its ATR-IR spectra (shown Fig. 10a) has some similarities with that for amorphous polymer (shoulders or bands at 1445, 1370, 1045, 900 cm^{-1}).

The C1s spectrum for untreated PET consists of three distinct peaks (without the peak due to $\pi - \pi^*$ shake up transition), similar with those presented in literature [19]: the carbon atoms in the benzene ring C_1 (285 eV), the methylene carbon singly bonded to oxygen C_2 (286.7 eV) and the ester carbon atoms C_3 (288.8 eV). Two peaks, due to the carbonyl O_1 (O=C, 532 eV) and ester O_2 (O—C, 533 eV) oxygen atoms are stood out in the O1s spectrum of the untreated PET. Resolved peak areas do not agree with the calculated carbon ratio, 3 : 1 : 1, the content in carbon singly bonded to oxygen C_2 being greater than the content in carbon double bonded to oxygen C_3, especially in a surface layer thinner than 30 Å. This behaviour can be explained knowing that in a paracrystalline structure, like in PET foils, the spaces between crystallites are completed with an amorphous phase which is determined by the chaotically and homogeneous distribution of the $-CH_2-$ groups. The difference of almost 10% in the intensities for O_2 and O_1 in the untreated PET could be due to the presence of some residual monomer or to the cyclic oligomers [12].

The untreated PET has a hydrophobic (with a low value for non-dispersive, or acid-base component $\gamma_s^{ab} = 2.2$ mN/m) and amphoteric ($\gamma_s^+ = \gamma_s^- = 1.1$ mN/m) surface.

Surface Energy Data

The sessile drop measurements were made both immediately after treatment and at various time intervals after the treatment. These last measurements were made to stand out the so called "ageing" effect.

The values of the acid-base component ($\gamma_s^{ab} = \gamma_s^+ + \gamma_s^-$) correspondent for PET treated in IB-LDP system are higher in respect with those obtained for the untreated sample ($\gamma_s^{ab} = 2.2$ mN/m), no matter the dose and the energy of the ions are (Tab. III). The increase of the acid-base component could be an indication of functional groups introduction into the surface exposed to the ion bombardment, the number of these ones being higher, higher the dose and the energy of the ions are.

Acid γ_s^+ and base γ_s^- surface energy components vs. ion energy and dose (as they were measured immediately after treatment) are represented in Figure 3, in which arrows mark the values for untreated sample. For treatments with 100 eV ions, both γ_s^+ and γ_s^- increase at δ_1, but at higher doses slightly depend (increase) on δ. Treatments with oxygen ions of 300 eV increase γ_s^+, excepting at the lowest dose when this one is slightly diminished as comparing with untreated PET (Fig. 3a), while γ_s^- has greater values than for the initial PET, for all doses, with a lower value for δ_2-300 sample (Fig. 3b). Extremely different dependencies γ_s^+ and γ_s^- versus δ are shown for samples treated with 500 eV ions. γ_s^+ obviously increases for samples treated at δ_1 and δ_2, while at δ_3 it decreases around the value for untreated sample (Fig. 3a). γ_s^- increases with δ up to 23 mN/m at δ_3 (Fig. 3b).

The evolution of γ_s^{ab} (Tab. III), γ_s^+ (Fig. 4) and γ_s^- (Fig. 5) with the ageing time stand out some common features. More or less decreasing of γ_s^{ab}, γ_s^+ and γ_s^- with the ageing time is observed, which is the general trend stood out for polymers treated in RIBE or IBE system

TABLE III Acid-base component of the surface free energy for PET samples treated in IB-LDP system

Sample	γ_s^{ab} (*mN/m*) *ageing time* (*days*)			
	0	*1*	*3*	*7*
δ_1-100	6.4	7.2	6.0	17.5
δ_2-100	8.3	7.6	7.0	6.5
δ_3-100	9.1	9.5	8.3	11.2
δ_1-300	5.6	4.5	5.6	9.8
δ_2-300	7.2	4.7	5.0	5.2
δ_3-300	12.3	10.4	9.6	12.4
δ_1-500	6.5	5.9	4.6	5.7
δ_2-500	12.4	6.8	12.7	11.7
δ_3-500	24.3	15.1	10.2	10.0

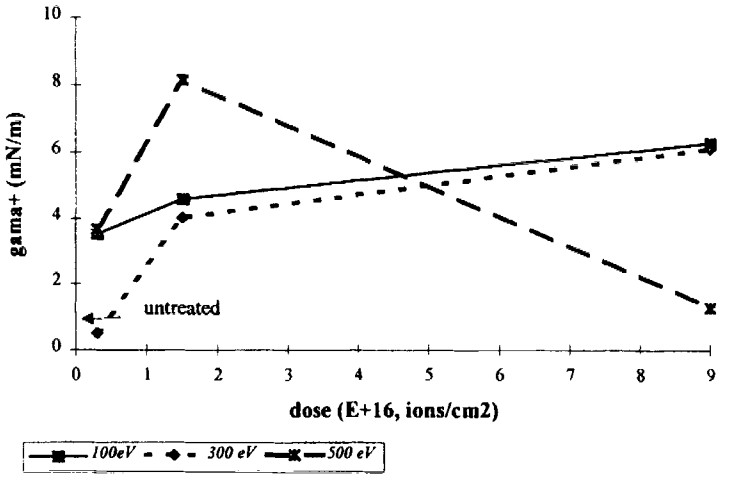

a.

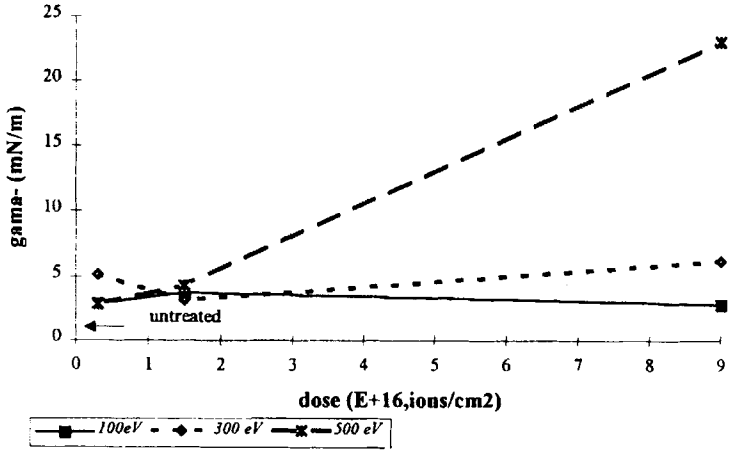

b.

FIGURE 3 a) Acid γ_s^+ and b) base γ_s^- component of the surface energy vs. oxygen ion energy and dose.

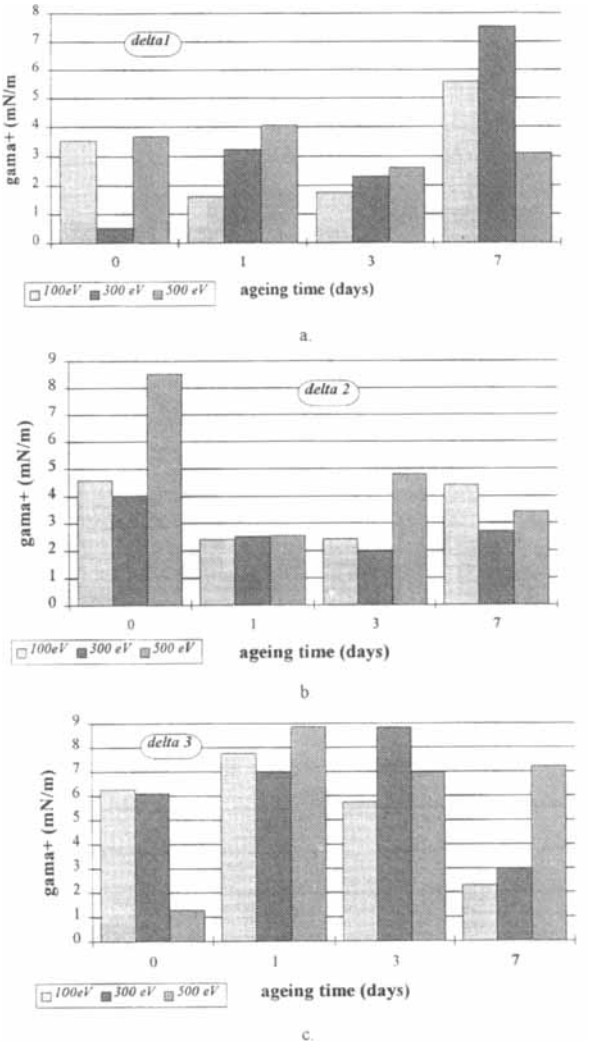

FIGURE 4 Evolution of γ_s^+ with "ageing time" for PET samples treated at: a) δ_1, b) δ_2 and c) δ_3.

[7, 9, 11]. These evolutions are function of the treatment conditions being different even in the case when the initial (immediately after the treatment) values are comparable. For example, the samples δ_1-100

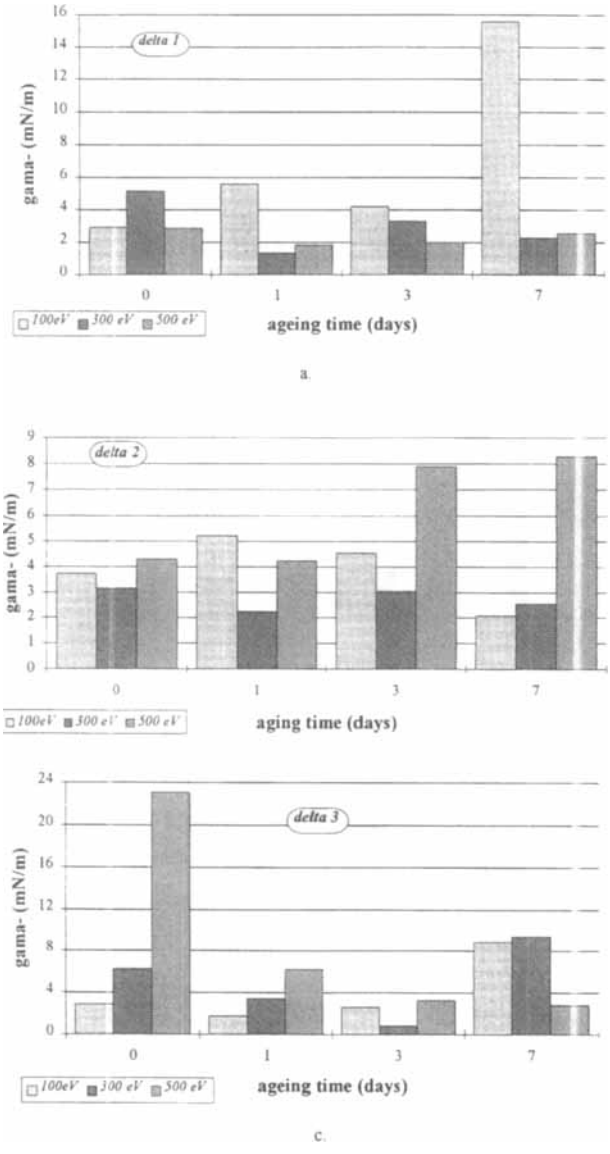

FIGURE 5 Evolution of γ_s^- with "ageing time" for PET samples treated at: a) δ_1, b) δ_2 c) δ_3.

and δ_1-500 has almost the same initial values for γ_s^{ab} (Tab. III) and also for γ_s^- (Fig. 5), but evolution in time stand out different dynamic surface effects for the two samples.

γ_s^{ab} increase seven days after the treatment (as comparing with the values obtained immediately after the treatment) for the samples treated with ions of 100 and 300 eV, at the lowest dose. This increase is higher lower is the ion energy (Tab. III). For δ_1-100 this increase is due mainly to the increase in γ_s^- (Fig. 5a) while for δ_1-300 to the increase in γ_s^+ (Fig. 4a). Such unexpected feature was also observed by Brennan and co-workers for oxygen plasma treated PEEK [8].

The total polar group content is more stable as the energy and dose increase with an exception for δ_3-500 sample. Therefore γ_s^{ab} is almost unchanged for δ_3-100, δ_3-300, δ_1-500 and δ_2-500 (Tab. III).

On the other hand, data for γ_s^+ and γ_s^- evolution with the ageing time show two main aspects. Firstly, the samples with an initial pregnant surface acidic character like δ_3-100, δ_3-300 and δ_2-500 (Fig. 4, 0 days after treatment) evolve to a pregnant basic one (Fig. 5, 7 days after treatment); conversely, the sample δ_3-500 with a pregnant basic character immediately after the treatment (Fig. 5c, 0 days after treatment) evolves to an acidic one (Fig. 4c, 7 days after treatment). Secondly, samples which do not present a prevalent acidic or basic character (like δ_2-100, δ_2-300, δ_1-500) are more stable in time (show no important modification in their acid or base surface component). These aspects are very important for practical purpose of such modifications.

Without giving at this moment an explanation of the above presented surface energetic data it must briefly pointed out few aspects concerning the dynamic surface effects, as are presented in the literature [8, 9, 20]. The increase in the surface concentration of hydrophilic or hydrophobic groups leads to highly asymmetric surface structure, which in turn causes much stress and many different stress-induced mechanisms as: outdiffusion of untreated subsurface molecules through the modified layer, short range reorientation of macromolecular segments or side chains, chemical reactions between introduced groups and surroundings or the chemical groups of the parent polymer. The short range monomeric or segmental motion such as the rotation of a side chain around a carbon–carbon bond (β relaxation), take place within the modified layer, leading to burial of

polar group away from the surface. This mechanism is expected independent of molecular weight. The long range motion and out diffusion of untreated molecules is much more demanding intense of activation energy and it has a strong dependence on molecular weight. While minor effects were observed in the short range recovery mechanisms, the onset of recovery by long range mobility was lowered, the lower cross-linking [8, 9]. Therefore, two main conditions must be fulfilled to reduce the recovery mechanism: a maximum amount of oxygen introduced on the surface, which interact by hydrogen bonding and a higher reticulated content [20].

Values for γ_s^+ and γ_s^-, seven days after the treatment, are given in Figure 6, to show more clear the predominant acidic or basic surface character of each sample. Samples which have mainly basic character are: δ_1-100, δ_3-100, δ_2-500 and δ_3-300, while those which have acidic character are δ_1-300 and δ_3-500. The others do not present a prevalent acid or base character.

XPS Data

It must pointed out that XPS data were obtained after more than a month from the treatment and these data could be corroborated only

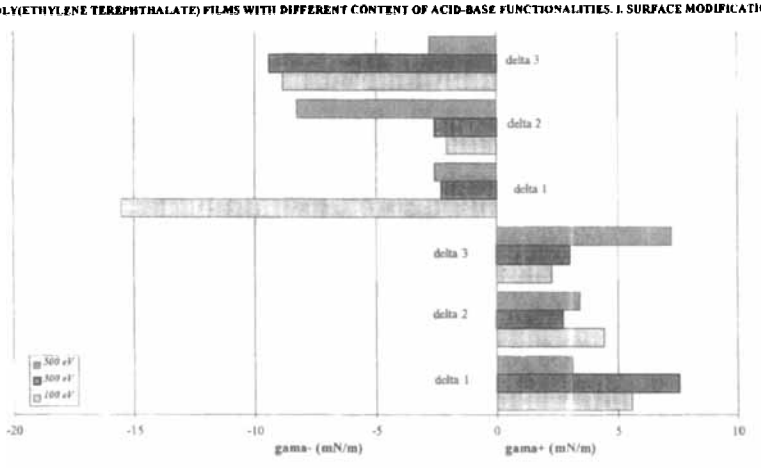

FIGURE 6 Diagram with γ_s^+ and γ_s^-, seven days after the treatment of PET samples.

with the surface energy data obtained seven days after the treatment. Even in this case a straight correlation between the values of the surface energy components and XPS data is difficult to get through. That since, as it is well known, the sessile drop measurements give information about chemical structure for the uppermost layers, while the XPS signal for a given species integrates across a layer of few tens angstroms. When such a correlation is an obvious one this could be a sign that induced modifications are the same in the uppermost and in the deeper layers.

PET samples were stored in closed vessel, in air, under normal conditions of temperature and humidity.

Different carbon contents as percentages from the total carbon [C_x] are given in Table IV as a function of treatment conditions and electron take off angle (or sampling depth). O1s/C1s, O—C/C and O=C/C atomic ratios as function of photoelectron take-off angle are given in Figures 7, 8 and 9, for samples treated at different ion energies and doses. In these figures arrows mark the correspondent values for untreated PET at 22.5°, 37.5° and 52.5° electron take-off angles.

Treatments with 100 eV ions do not appreciable modify [C_1], while [C_2] increases (especially at the highest dose) and [C_3] decreases for all investigated sample depth (Tab. IV), as comparing with untreated sample. O1s/C1s is smaller with 6–8% than for pristine polymer, in layers of about 30–50 Å of the δ_1-100 sample (Fig. 7a). A slight diminished O1s/C1s ratio is stood out in δ_2-100 sample, only in the superficial layers, while an important decrease of about 12% is shown in the profoundness of δ_3-100 sample. Decrease in O1s/C1s ratio is due to the decrease in O—C/C, for all doses (Fig. 7b). The decrease in O—C/C, concomitantly with a slight increase in O=C/C (Fig. 7c) (as comparing with the values for untreated PET), can explain basic (donor) character of δ_1-100 and δ_3-100 samples.

Treatments with 300 eV Ions

[C_1] increases especially for δ_2-300 and δ_3-300 samples. [C_2] doesn't change, while [C_3] decreases with 3–6% as compared with untreated sample (Tab. IV). The O1s/C1s ratio has a decrease of about 8–9%, for

TABLE IV $[C_x]$ ($\%C_{total}$) for different treated PET samples vs. sampling depth (electron take-off angle)

Sample		*Electron take-off angle (dgr.)*						
		22.5	*27.5*	*32.5*	*37.5*	*42.5*	*47.5*	*52.5*
untreated	$[C_1]$	56,6			60,3			60,0
	$[C_2]$	25,2			21,3			23,9
	$[C_3]$	18,2			18,3			15,9
δ_1-100	$[C_1]$	58,8	59,2	60,6	60,9	61,7	63,3	62,9
	$[C_2]$	27,0	26,6	26,1	26,3	25,9	26,3	26,1
	$[C_3]$	14,1	14,2	13,2	12,8	12,3	10,3	11,0
δ_2-100	$[C_1]$	57,8	54,5	59,1	60,9	58,3	60,2	60,2
	$[C_2]$	26,5	30,0	26,6	25,6	25,6	26,5	26,5
	$[C_3]$	15,6	15,4	14,2	13,4	16,0	13,2	13,2
δ_3-100	$[C_1]$	55,5	58,3	56,8	58,8	58,2	57,8	61,9
	$[C_2]$	29,4	27,8	30,7	28,2	28,7	28,9	29,5
	$[C_3]$	14,9	13,9	12,5	12,9	13,0	13,3	8,5
δ_1-300	$[C_1]$	59,7	63,1	62,5	61,7	64,1	62,1	62,5
	$[C_2]$	26,8	23,9	26,2	25,9	24,3	26,7	26,2
	$[C_3]$	13,4	12,8	11,2	12,3	11,5	11,2	11,2

δ_2-300	[C_1]	61,8	60,2	61,7	63,7	62,9	66,6	63,3
	[C_2]	26,2	26,5	25,9	25,5	24,5	23,3	25,3
	[C_3]	11,9	13,2	12,3	10,8	12,6	9,9	11,4
δ_3-300	[C_1]	62,2	60,2	61,7	64,6	64,5	63,7	68,6
	[C_2]	25,4	25,3	25,9	23,8	25,1	23,5	21,8
	[C_3]	12,4	14,4	12,3	11,6	10,3	12,7	9,5
δ_1-500	[C_1]	61,0	63,7	62,8	62,3	63,3	65,8	70,5
	[C_2]	26,7	23,5	24,5	25,1	24,0	22,8	18,2
	[C_3]	12,2	12,7	12,6	12,6	12,6	11,4	11,2
δ_2-500	[C_1]	59,2	59,8	60,2	62,5	62,5	62,5	64,5
	[C_2]	25,4	25,1	25,3	24,9	26,2	26,2	24,5
	[C_3]	15,3	15,1	14,4	12,5	11,2	11,2	10,9
δ_3-500	[C_1]	56,9	58,4	59,2	62,1	61,7	60,9	64,6
	[C_2]	28,3	27,5	27,2	24,8	27,2	26,8	26,4
	[C_3]	14,7	14,1	13,6	13,0	11,1	12,2	9,0

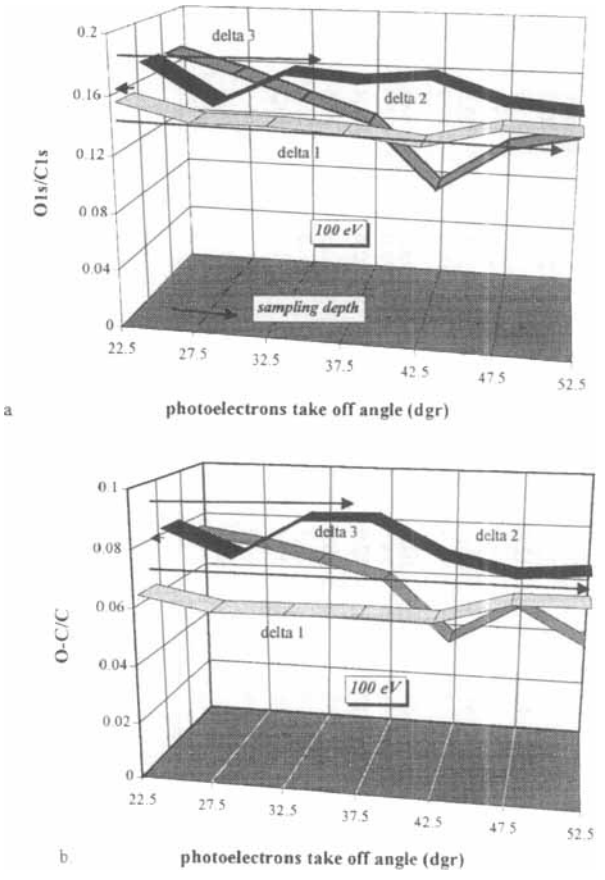

FIGURE 7 Values of: a) O1s/C1s, b) O—C/C and O=C/C ratios vs. electron take-off angle (sampling depth), for samples treated with 100 eV ions, at different doses.

all investigated sample depths in δ_1-300 sample (Fig. 8a), decrease due both to diminishing in O—C/C (Fig. 8b) and O=C/C (Fig. 8c) ratios. Almost unchanged value of O1s/C1s ratio for δ_2-300 sample is the result of the decreased O—C/C and increased O=C/C. The increased O1s/C1s for δ_3-300 sample is duc to increasing in both O—C/C and O=C/C. It must also stood out an extremely uniform depth profile for the values of these ratios for all samples treated with 300 eV ions. XPS data doesn't

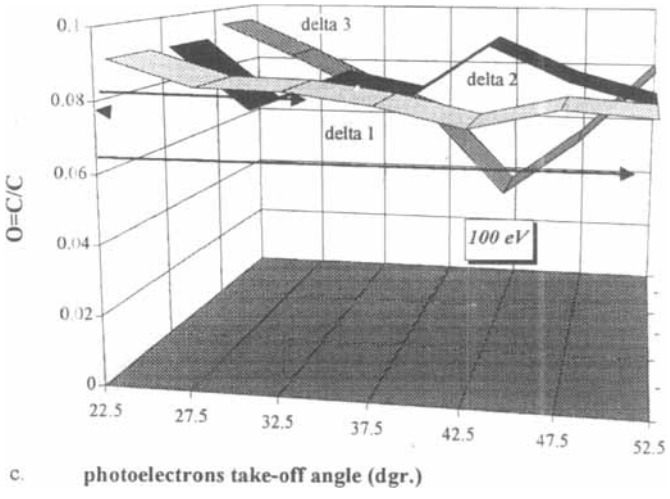

c.

FIGURE 7 (Continued).

POLY(ETHYLENE TEREPHTHALATE) FILMS WITH DIFFERENT CONTENT OF ACID-BASE FUNCTIONALITIES. I. SURFACE MODIFICATIONS

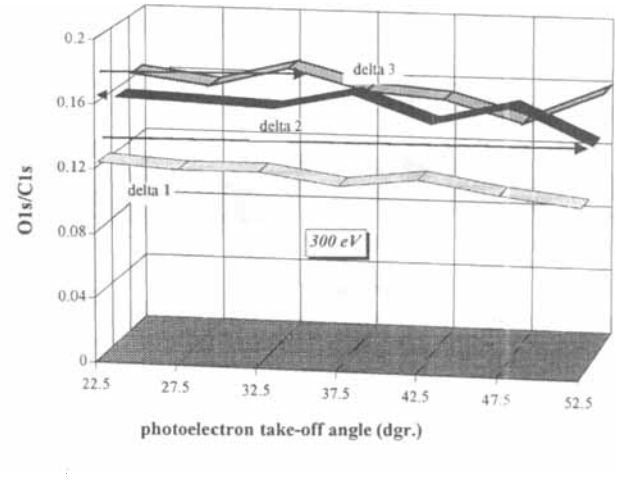

a.

FIGURE 8 Values of: a) O1s/C1s, b) O—C/C and O=C/C ratios vs. electron take-off angle (sampling depth), for samples treated with 300 eV ions, at different doses.

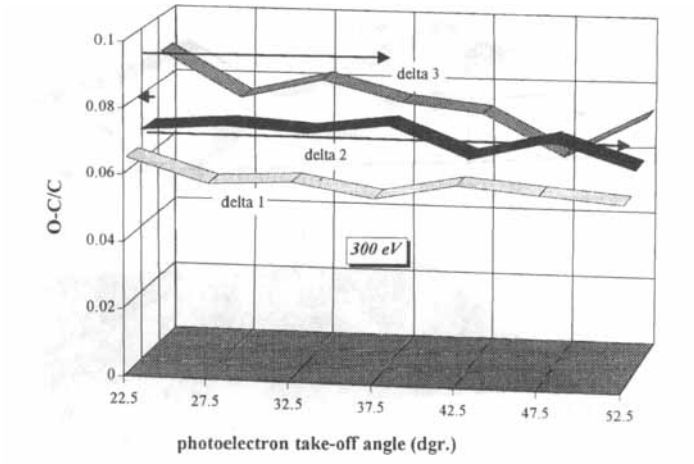

b.

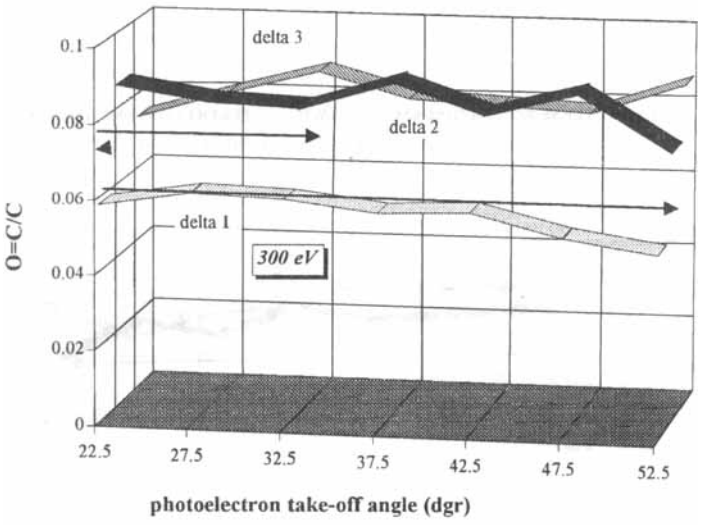

c.

sustain the surface energetic for these samples which suggests that the acidic or basic groups are mainly created in a thinner layer than the sampling depth for photoelectrons (even for the lowest value of α).

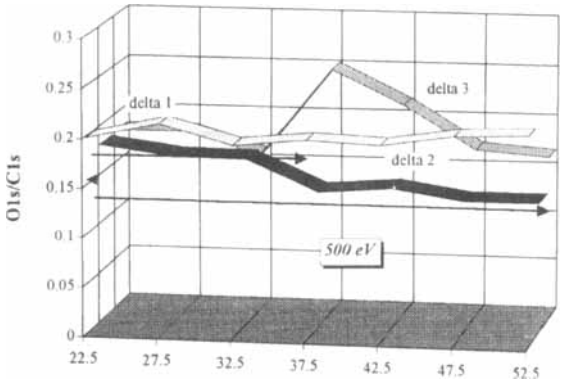

a.

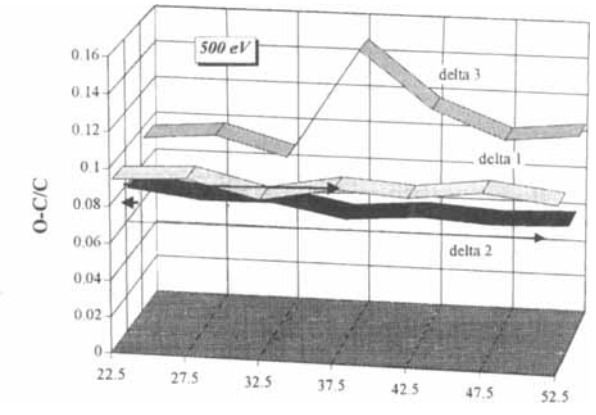

b.

FIGURE 9 Values of: a) O1s/C1s, b) O—C/C and O=C/C ratios vs. electron take-off angle (sampling depth), for samples treated with 500 eV ions, at different doses.

Treatments with 500 eV Ions

$[C_1]$ is increased, mainly in deeper layers and at low dose. $[C_2]$ has an increase in all investigated depths, only for δ_3-500 sample, while $[C_3]$

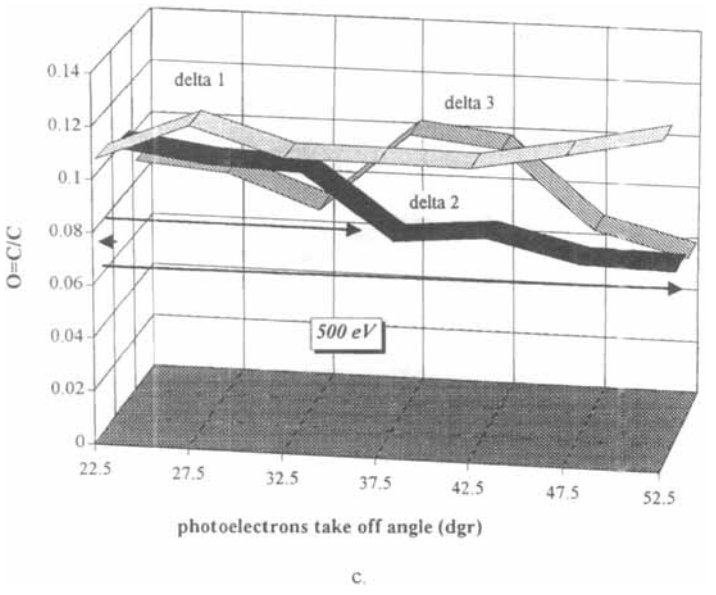

FIGURE 9 (Continued).

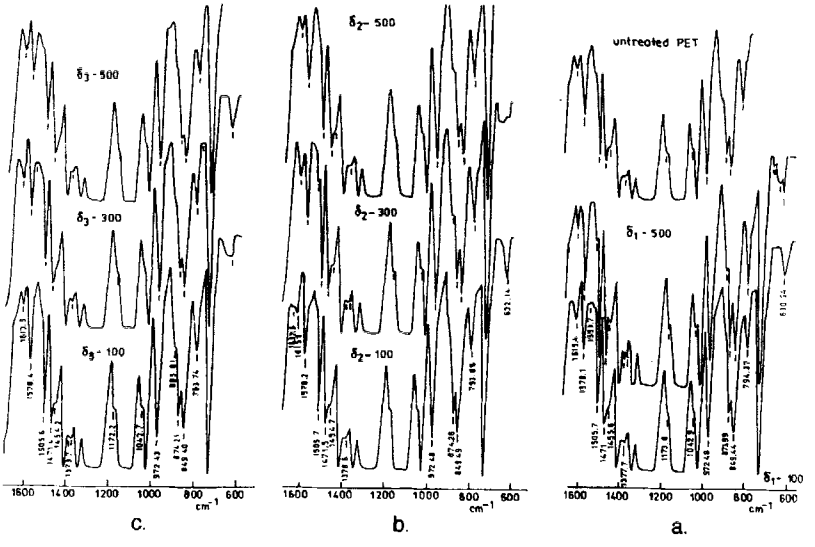

FIGURE 10 IR spectra for: a) untreated and treated PET at δ_1, b) δ_2 and c) δ_3.

decreases for all treated samples with 500 eV ions (Tab. IV). O1s/C1s increases with 18–20% for all investigated depths of δ_1-500 sample. The increase of about 5% for this ratio, for δ_2-500 sample, is stood out only in the superficial layers. For δ_3-500 sample O1s/C1s increases with $\approx 5\%$ in the uppermost layers and has a sharp increase of about 20% at a depth of around 50 Å (Fig. 9a). The increase of O1s/C1s, for samples treated at δ_1 and δ_2 is due to the increase of O=C/C, while for the sample treated at δ_3 is mainly due to O—C/C increasing (Figs. 9b and c). These data also sustained the surface energy data: δ_2-500 has a basic character, while δ_3-500 and acidic one.

IR Spectroscopy Data

It must pointed out that the treatments do not appreciable modify the film thickness.

Treatments at the Lowest Dose δ_1 (Fig. 10a)

Cis shoulders are appreciable diminished in δ_1-100 sample, but increased in δ_1-500 sample, as comparing with untreated PET. These features sustain a decrease and an increase respectively in amorphous content for the above mentioned samples. A diminishing of 1578 cm^{-1} band (due to ) is also observed in δ_1-100 sample, while the same band is increased in δ_1-500. For this last sample, the 973 cm^{-1} band, due to CH—benzenic is increased as comparing with untreated PET sample.

Treatments at the Medium Dose δ_2 (Fig. 10b)

IR spectra for δ_2-100 sample is similar with that for δ_1-100. Bands corresponding to *cis* phase are increased in δ_2-300, but obviously diminished in δ_2-500 as comparing with untreated sample. For the same samples 1578 cm^{-1} peak is increased.

Treatments at the Highest Dose δ_3 (Fig. 10c)

Cis shoulders are extremely diminshed and even vanished in δ_3-300, but especially in δ_3-500 sample. The 1570 cm^{-1} and 872 cm^{-1} bands are diminished in the same samples.

The above mentioned results suggest important modifications in amorphous and crystalline content of the oxygen ion beam treated PET. Such modifications will be stood out also by X-ray diffraction.

X-ray Diffraction Data

The X-ray diffraction at wide angles (Tab. V and Fig. 11) shows that generally, the main (100) peak doesn't modify his position (θ) or the width at 50% maximum intensity (β). This means that ions do not significantly change (in the bulk of the sample) the degree of ordering due mainly to the preferred orientation of the benzene rings in the specimen plane. However, some modifications appear, especially at higher ion energies and doses.

Therefore, X-ray patterns of 100 eV treated samples are similar to that for untreated PET. Some additional small peaks appear at low angles, due (100) planes of CH_2 groups, especially in δ_3-100 sample (Fig. 11a). The amorphous halo is diminished with increasing dose, for 300 eV treated samples (Fig. 11b). A decrease in (100) peak intensity and also in crystallite size on the normal direction to the (100) plane (D) is stood out for δ_2-300. A decrease of D is stood out for δ_2-500 sample (Tab. V). The amorphous halo is slightly diminished in δ_2-500 samples (Fig. 11c).

The values for long period L, as were determined from small angle diffraction data, are given also in Table V. As comparing with untreated sample, L, which represents the medium distances from the crystalline domains [16], is slightly increased in δ_2-100, δ_3-100 and δ_3-500 and decreased in δ_3-300 and δ_1-500. This feature could be due to

TABLE V X-ray diffraction data at wide angles for PET samples treated in IB-LDP system

Sample	θ(*dgr.*)	L(Å)	d(Å)	β(*dgr.*)	D(Å)
δ_1-100	15.04	40.2	3.4478	2.548	60.3
δ_2-100	15.04	42.7	3.4478	2.548	60.3
δ_3-100	15.04	41.0	3.4478	2.399	58.7
δ_1-300	15.04	39.4	3.4478	2.548	60.3
δ_2-300	15.02	39.4	3.4528	2.315	58.2
δ_3-300	15.01	37.4	3.4550	2.389	58.6
δ_1-500	15.04	35.4	3.4478	2.375	60.3
δ_2-500	15.04	39.4	3.4478	2.311	55.7
δ_3-500	15.04	42.7	3.4478	2.414	60.3

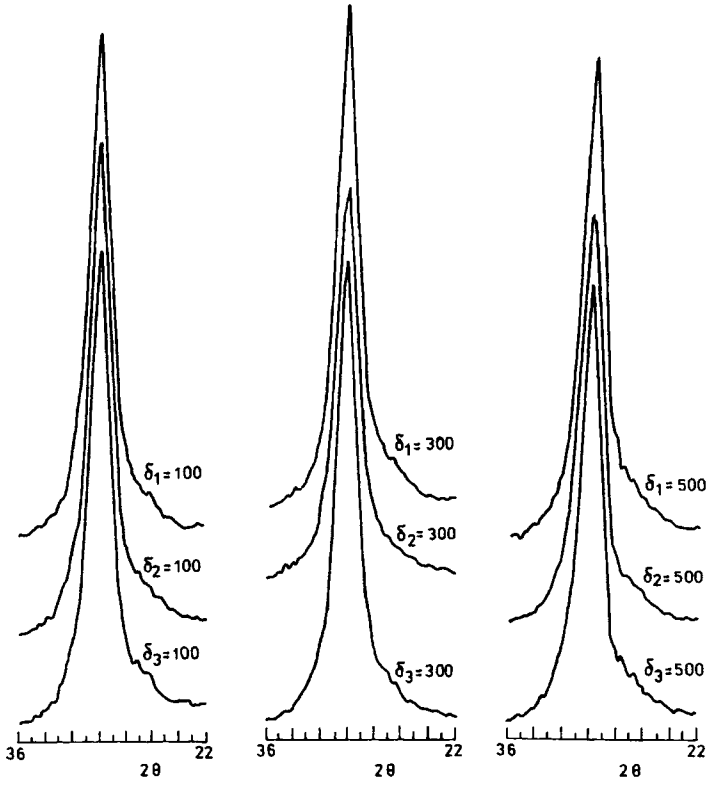

FIGURE 11 X-ray patterns for PET samples treated with ions of: a) 100 eV, b) 300 eV and c) 500 eV.

two competitive processes: one which induced distortions in crystallite structure and other a recrystallization process.

In Figures 12 are given the main peak (100) intensities, as functions of ion energy and dose, for three values of the incident angles ω. The arrow marks the (100) peak intensity for untreated PET, at the same ω. Generally, oxygen ion beam treatments of PET determine the increase in number of (100) planes which make angles different from zero with the sample surface plane, $N_{(100)\text{-}\omega}$. The number of planes which make a relative large angle with sample surface, $N_{(100)\text{-}4}$, increases with δ for 300 eV ion energy treated samples, but do not depend on δ for 100 eV and 500 eV treated PET samples (Fig. 12a). $N_{(100)\text{-}6}$ is prominent increased when it is pass from saturation to reimplantation regime of

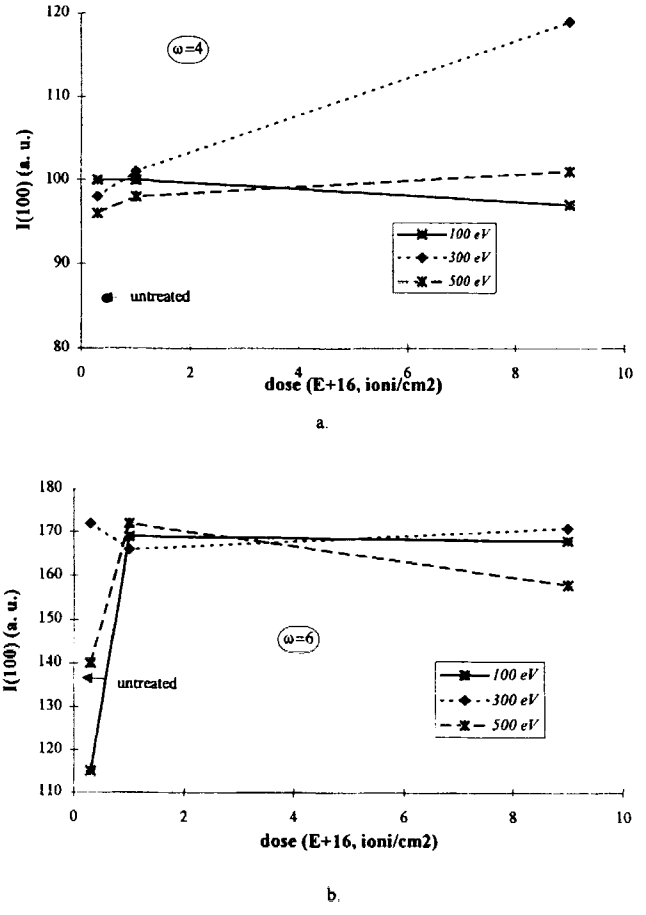

FIGURE 12 Intensity of (100) peak vs. treatment dose and ion energy for: a) $\omega = 4°$, b) $\omega = 6°$ and c) $\omega = 8°$.

dose, for ion energy of 100 eV and 500 eV; it does not depend on δ for samples treated with 300 eV ion energy (Fig. 12b). $N_{(100)\text{-}8}$ does not depend on dose for samples treated with ions of 100 eV, is diminished for δ_3-300 sample and tends to saturate with dose for samples treated with ions of 500 eV.

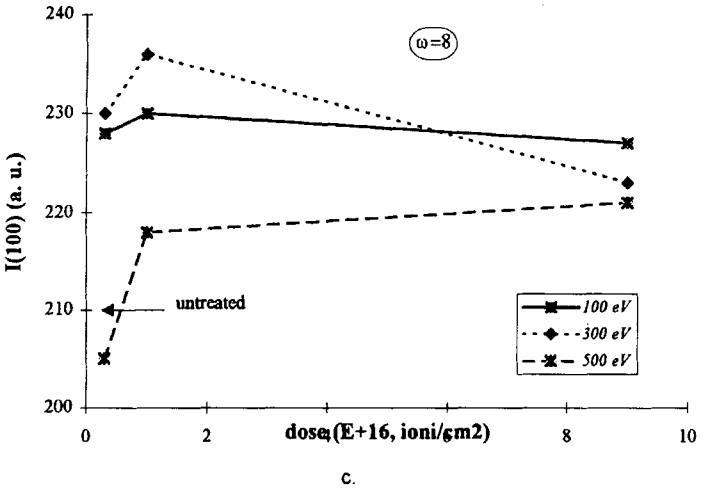

c.

FIGURE 12 (Continued).

CONCLUSIONS

Since a tentative explanation of the mechanisms involved in the above mentioned surface modifications will be presented in the second part of this paper, after the presentation of the results on the plasma gas-phase analysis, now there will be pointed out only few important aspects.

Both chemical and physico-structural modifications take place simultaneous during ion beam treatments and treated samples' ageing.

The introduction of the oxygen functionality in the PET surface, stood out by the values for γ_s^{ab} and those for γ_s^+ and γ_s^-, starts for the samples treated at the lowest dose δ_1. However, the content in such functionality is not one which could award a prevalent surface acidic or basic character for the samples treated at this lowest dose.

The acidic functionality contents increases with treatment dose, at the same ion energy, while the basic ones are not too much influenced by the treatment dose. The δ_3-500 sample is an exception having a very high value for γ_s^- and a diminished value, closed to that for untreated PET, for γ_s^+.

The initial polar group content (immediately after the treatment), but more than this the physico-structural modifications like

cross-linking and a restructured crystalline content (stood out by IR spectra and X-ray diffraction at grazing incidence geometry) determine the dynamic effects.

References

[1] Fowkes, F. M. (1987). *J. Adhesion Sci. Technol.*, **1**, 7.

[2] Mittal, K. L. (1975). In "Adhesion Science and Technology", L. H. Lee, Ed., Part A, Plenum Press, New York.

[3] a) K. L. Mittal and J. R. Susky Eds., (1989). In "Metallized Plasctics 1: Fundamental and Applied Aspects", Plenum Press, New York; b) Galuska, A. (1992). In "Metallized Plasctics 3: Fundamental and Applied Aspects", K. L. Mittal Ed., Plenum Press, New York p. 267; c) Cain, S. R. (1991). In "Acid-Base Interac-tions", K. L. Mittal and H. R. Anderson Eds, VPS, Utrecht, p. 47.

[4] a) Fowkes, F. M., McCarthy, D. C. and Tischles, D. O. (1985). In "Molecular Characterization of Composite Interface", H. Ishida and G. Kumar Eds, Plenum Press, New York, p. 401; b) Dwight, D. W., Fowkes, F. M., Cole, D. A., Kulp, M. J., Sabat, P. J., Salvati, L. and Huang, T. C. (1991). In "Acid-Base Interactions", K. L. Mittal and H. R. Anderson Eds, VPS, Utrecht, p. 243.

[5] a) Ruckenstein, E. and Sathyamurthy, V. (1984). *J. Coll. Interf. Sci.*, **101**, 436; b) Jozefonvicz, J. and Jozefowicz, M. (1992). *Pure and Appl. Chem.*, **64**(1), 1783; c) Gheorghiu, M., Popa, G. and Mungiu, O. (1991). *J. Bioact. Compat. Polym.*, **6**, 164.

[6] Munro, H. S. and McBrian, D. I. (1988). *J. Coating Technol.*, **60**, 41.

[7] Morra, M., Occhiello, E. and Garbassi, F. (1989). *J. Colloid Interf. Sci.*, **132**, 504.

[8] Brennan, W. J., Feast, W. J., Munro, H. S. and Walker, S. H. (1991). *Polymer*, **32**, 527.

[9] Morra, M., Occhiello, E. and Garbassi, F. *Proc. of the 1-st Int. Conference*, Namur, Belgium, 1991, Sec. IV, p. 407.

[10] Tatoulian, M., Arefi-Khonsari, F., Rouger, I., Amouroux, J., Gheorghiu, M. and Bouchier, D. (1995). *J. Adhesion Sci. Technol.*, **9**(7), 923.

[11] Gheorghiu, M., Placinta, G., Arefi, F., Amouroux, J., Tatoulian, M. and Popa, G. (1997). *Plasma Sources Sci. and Technol.*, **6**, 8.

[12] Gheorghiu, M., Rusu, I. and Popa, G. (1996). *Vacuum*, **47**(9), 1093.

[13] Marletta, G. (1990). *Nucl. Instrum. and Meth.*, **B 46**, 295.

[14] Wu, S. (1982). In "Polymer Interface and Adhesion", Marcel Dekker Ed., New York.

[15] Vrabanac, M. D. and Berg, J. C. (1991). In "Acid-Base Interactions. Relevance to Adhesion Science and Technology", K. L. Mittal and H. R. Anderson Eds., VPS, Utrecht, p. 67.

[16] Fourche, G. (1995). *Polym. Eng. and Sci.*, **35**(12), 957.

[17] Benisch, J., Hollander, A. and Zimmermann, H. (1993). *J. Appl. Polymer Sci.*, **49**, 117.

[18] Alexander, L. E. (1969). In "X-Ray Diffraction Methods in Polymer Science", Wiley J. and Sons.

[19] Clark, D. T. and Dilks, A. (1978). *J. Polym. Sci. Polym. Chem. Ed.*, **16**, 911.

[20] Garbassi, F., Occhielo, E., Morra, M., Barino, L. and Scordamaglia, R. (1989). *Surf. Interf. Anal.*, **14**, 595.